

## Note

---

### Triple-stranded, left-hand-twisted cellulose microfibril\*

GEORGE C. RUBEN\*\*,

*Department of Biology, Dartmouth College, Hanover, NH 03755 (U.S.A.)*

AND GORDON H. BOKELMAN

*Philip Morris Research Center, P.O. Box 26583, Richmond, VA 23261 (U.S.A.)*

(Received March 17th, 1986; accepted for publication in revised form, October 6th, 1986)

Because the crystal structure cellulose I is, from X-ray work, modeled as parallel chains of (1→4)- $\beta$ -D-glucan organized in parallel, off-set planes<sup>1–3</sup>, it is generally assumed that the units of cellulose synthesis can fasciate laterally along crystallographic lattice planes, forming microfibrils of a range of thicknesses and crystallite sizes. The width of the cellulose crystallites has been estimated from the equatorial X-ray fiber diffraction line broadening<sup>4,5</sup>, which gives crystallite widths of 65–75 Å in *Acetobacter xylinum*<sup>5,6</sup>, and larger crystallites in other organisms<sup>4,5,7</sup> (100–200 Å). These sizes have been generally assumed to be the microfibril width.

Submicrofibrils of 10–20 Å, or microfibrils of 35 Å, or both, have been seen by transmission electron microscopy (TEM) in ramie<sup>8,9</sup>, jute<sup>9</sup>, cotton<sup>9</sup>, *A. xylinum*<sup>6,10–14</sup>, quince<sup>15</sup>, wood<sup>16</sup>, and rose<sup>17</sup>. Although this evidence should be significant, the concept of lateral fasciation has been invoked to explain how negative staining or prior treatment, or both, or sonication of larger crystallites, has separated them into smaller fibrils<sup>4,5,14,18</sup>.

We shall show by high-resolution Pt–C replication, a method which has resolved<sup>19,20</sup> the helix features of DNA, that there are, within the 36.8-Å microfibril, three 17.8-Å submicrofibrils that are twisted in left-handed fashion around its axis. Because the surfaces of the longitudinal axis of the microfibril are not single lattice planes as previously modeled, the concept of lateral fasciation along corresponding crystallographic planes (fusing to form thicker microfibrils) is no longer feasible.

## EXPERIMENTAL

The tobacco lower epidermal peels were prepared from a Coker 319 leaf

---

\*Presented at the 44th annual meeting of the Electron Microscopy Society of America, Albuquerque, NM, August 10–15, 1986.

\*\*To whom correspondence should be addressed

(No. 13 on stalk). These peels were immersed in 1:3 ethanol–water blotted to remove the excess solution and then frozen on 1.25-cm mica discs by rapid immersion in liquid propane ( $-190^{\circ}$ ). This sample was freeze-dried for 3 h at  $-70^{\circ}$ , and then replicated with 15.9 Å Pt–C ( $45^{\circ}$  angle) at  $-178^{\circ}$  *in vacuo* (6.67  $\mu$ Pa) and backed with 139 Å of carbon, (Wiltek Industries modified Balzer's 301 with cryopump and rebuilt cold stage<sup>21</sup>).

The *A. xylinum* was grown on 40mM D-glucose and 5M phosphate (pH 7,  $20^{\circ}$ ) until it formed a white, flocculent surface cap on the solution. Samples prepared in this way were then grown consecutively on 25 $\mu$ M Tinopal for 1 h, on 0.25mM Tinopal for 1.5 h, on 25 $\mu$ M Tinopal for 1 h, and then on 40mM D-glucose and 0.5M phosphate (pH 7,  $20^{\circ}$ ) for 1 h. Each cohesive mass of cellulose with cells growing at its periphery was sequentially rinsed in 5 separate dishes of water followed by sequential rinsing in 5 separate dishes of 1:3 ethanol–water. Each sample was placed on a 1.25-cm Whatman 50 filter paper disc, blotted, and frozen in liquid propane. *A. xylinum*, grown normally was freeze-dried for 1.5 h at  $-78^{\circ}$ , then replicated with 17.3 Å Pt–C (at  $-178^{\circ}$ ), and backed with 90.2 Å carbon. The Tinopal-treated sample was freeze-dried for 2.8 h at  $-70^{\circ}$ , replicated with 16.4 Å Pt–C (at  $-178^{\circ}$ ), and backed with 156 Å of carbon. The *A. xylinum* treated with boiling trifluoroacetic acid was frozen in 1:3 ethanol–water, freeze-dried for 2 h at  $-70^{\circ}$ , replicated with 15.2 Å Pt–C, and backed with 173 Å of carbon. All of the samples were digested in 80% sulfuric acid. The replicas were rinsed in de-ionized water and then picked up with carbon-coated, 300-mesh grids from underneath and examined on a JEM 100CX instrument as described previously<sup>22</sup>. Indirectly evaporated carbon films<sup>22</sup> of  $\sim 80$  Å thickness, suspended on 300-mesh grids, were used to support *A. xylinum* cellulose that had been treated with boiling trifluoroacetic acid to remove hemicellulose. This sample was negatively stained with 2% uranyl acetate at pH 3.8.

To contrast-enhance unidirectional 15–18 Å thick Pt–C-coated cellulose specimens backed with 100–173-Å thick carbon films, micrographs were contrast-reversed on Kodak 7302 fine-grain, positive film<sup>22</sup>. In addition to increasing the contrast of 10–20-Å features, the Pt–C-coated surfaces are now white, and the molecular details are modulated on this background in blacks and shades of grey for easy structural interpretation<sup>19,20,23–25</sup>. By shooting a tilt series at  $10^{\circ}$  intervals at  $10^5\times$  on a JEM 100CX at 80 kV with a 5-mm focal length and a 40  $\mu$ m objective aperture, a 6.6-Å resolution and a 2710 Å depth of field are achieved in the picture series<sup>22</sup>. The tilt series is generally viewed stereoscopically, and then a single image representing the 3-D structure is shown, in order to estimate the real size of a filament underneath its Pt–C coating (unidirectional at a  $45^{\circ}$  angle), the longitudinal axis of a filament has to be within  $10^{\circ}$  of the general shadow-direction on the replica surface, so that both sides of the filament are Pt–C coated. The filament should be roughly at a  $45^{\circ}$  angle with the Pt–C source (checked by stereoviewing), although filaments Pt–C-coated at approximately a  $90^{\circ}$  angle were only 1 Å smaller<sup>25</sup>. A series of fiber-width measurements that are made at image magnifi-

cations of 2–5 million, and that usually number less than 100, are averaged, and the Pt–C film thickness, measured on the quartz-crystal monitor, is subtracted from the average width, to give an estimate of the real filament diameter<sup>26</sup>. It has recently been found<sup>23–25</sup> that this width-correction method should be reduced by 1.5 Å. Spacings along a Pt–C-coated microfibril or submicrofibril, in contrast, should be directly related to uncoated fibril spacings.

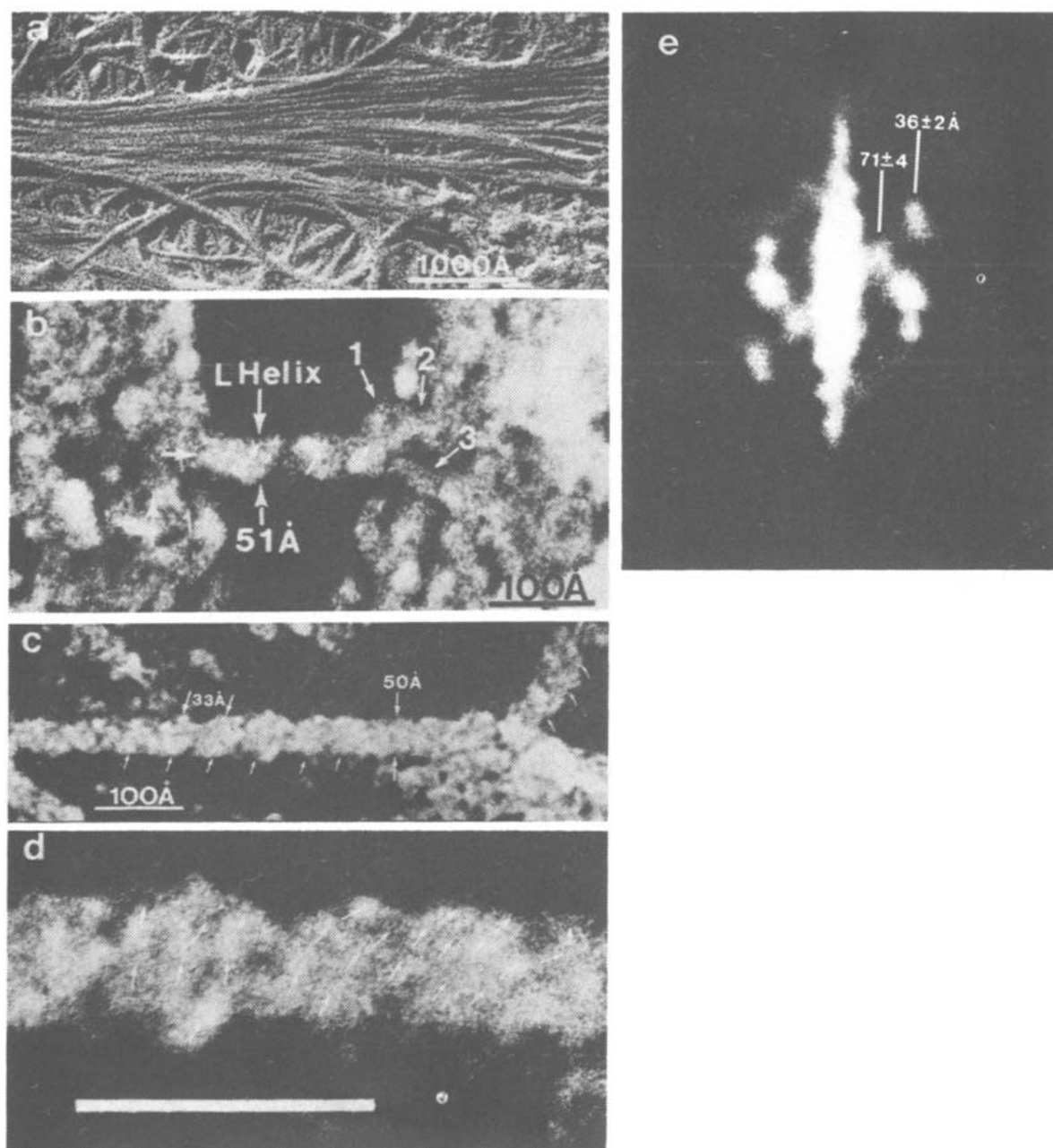


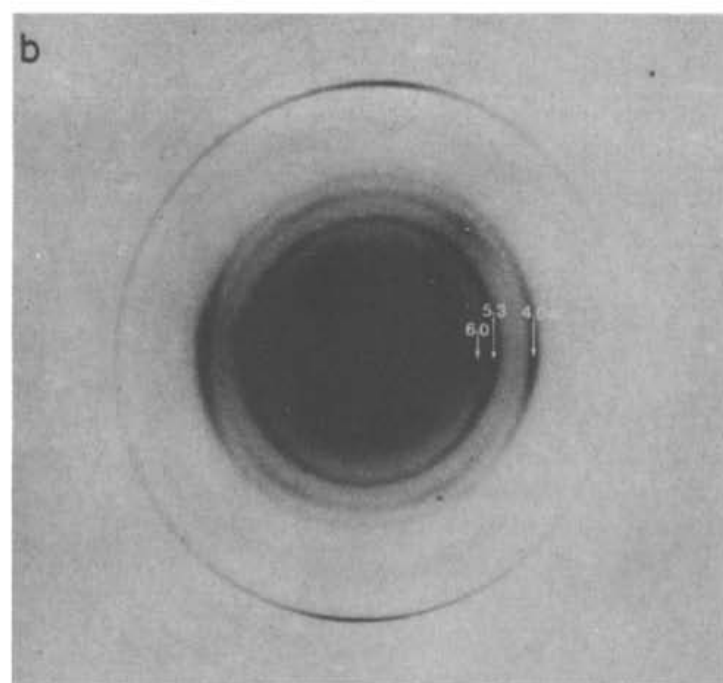
**Fig 1.** (a) Bundled array of cellulose microfibrils in lower epidermal cell-wall (facing mesophyll cells) of Coker 319 tobacco leaves. Epidermal peel was freeze-dried, Pt–C replicated (15.9 Å thick), and carbon-film backed. (b) Cellulose microfibril is seen connecting two bundled arrays of microfibrils (similar to those in Fig. 1(a)). This Pt–C-coated microfibril averages 51 Å in width, shows left-handed surface striations, and splits into three smaller submicrofibrils labeled 1, 2, and 3. (c) Tobacco primary cell-wall, Pt–C-coated microfibril averaging 50 Å shows left-handed surface striations at ~33 Å intervals. (d) Three 17–18 Å submicrofibrils in adjacent ridges wrap (see arrows) in a nonperiodic, left-handed fashion around the microfibril axis-bar, 100 Å. (e) Optical diffraction pattern of Fig 1(d); there are no left-handed, helical spacings. There are submicrofibril-surface spacings of  $71 \pm 4$  Å and  $36 \pm 2$  Å in the direction of their wrapping.

## RESULTS AND DISCUSSION

In Fig. 1(a), a freeze-dried, Pt-C-replicated, bundled array of parallel microfibrils is shown in the lower epidermal cell-wall of a Coker 319 tobacco leaf. In Fig. 1(b), one microfibril connects two microfibril bundles (similar to Fig. 1(a)). This

(a) Neutral sugars, after acid hydrolysis 51.4  
 (a) xylose 3.2% of total  
 (b) glucose 96.8% of total

(2) Protein content 30.0



C  
 C.p.-m.a.s.  $^{13}\text{C}$ -n.m.r. spectrum of cellulose I  
 (*Acetobactor xylinum*)

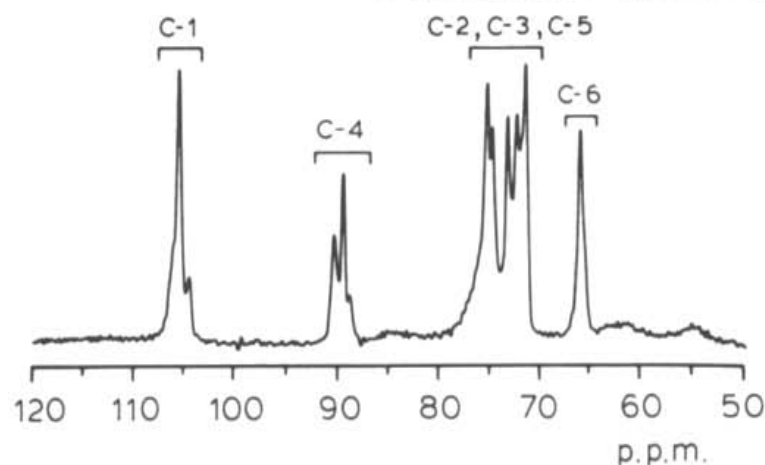


Fig. 2. (a) Chemical characterization of *A. xylinum* pellicle materials<sup>30</sup>. The predominant neutral sugar is, D-glucose, which is expected, as the pellicle is cellulose. Xylose is generally found in hemicellulosic materials<sup>1</sup>. (b) Electron diffraction pattern ( $c_1 = 46$  cm) of *A. xylinum* cellulose suspended over 100-mesh grid without a support film. Although 240 and 360-cm camera lengths were used, no spacings of about 33 Å or 17.8 Å could be detected. Nonetheless, normal equatorial cellulose I crystal spacings<sup>29</sup> of 6, 5.3, and 4 Å were recorded. (c)  $^{13}\text{C}$ -N.m.r. spectrum of dry *A. xylinum*, which demonstrates cellulose I spectrum previously reported<sup>27</sup>. Carbon atoms of the D-glucosyl monomer unit of cellulose are labeled.

microfibril shows left-handed, surface striations, and splits into three smaller submicrofibrils. Width correction for the Pt-C coating ( $15.9 \text{ \AA}$  thick) indicates a microfibrillar diameter of  $36.8 \pm 3 \text{ \AA}$ . Primary cell-wall microfibrils of the lower epidermis also show left-handed surface striations (see Fig. 1(c)). Such a microfibril exhibits periodic ridges and grooves at intervals of  $\sim 33 \text{ \AA}$ . At  $2.9 \times 10^6$  magnification (see Fig. 1 (d)), three  $17\text{--}18 \text{ \AA}$  submicrofibrils in three adjacent ridges are visible traversing (see arrows) the microfibril in a left-handed direction. The optical diffraction pattern in Fig. 1(e) is of the microfibril in Fig. 1(d). This pattern does not show any regular left-handed periodicities between the submicrofibrils, but it does show  $71 \pm 4 \text{ \AA}$  and  $36 \pm 2 \text{ \AA}$  surface periodicities along the  $17.8 \text{ \AA}$  submicrofibrils. We shall return to this point later.

Native cellulose I from *A. xylinum* also forms a three-stranded, left-handed helicoidally wrapped microfibril. We have demonstrated by examination of a  $^{13}\text{C}$ -

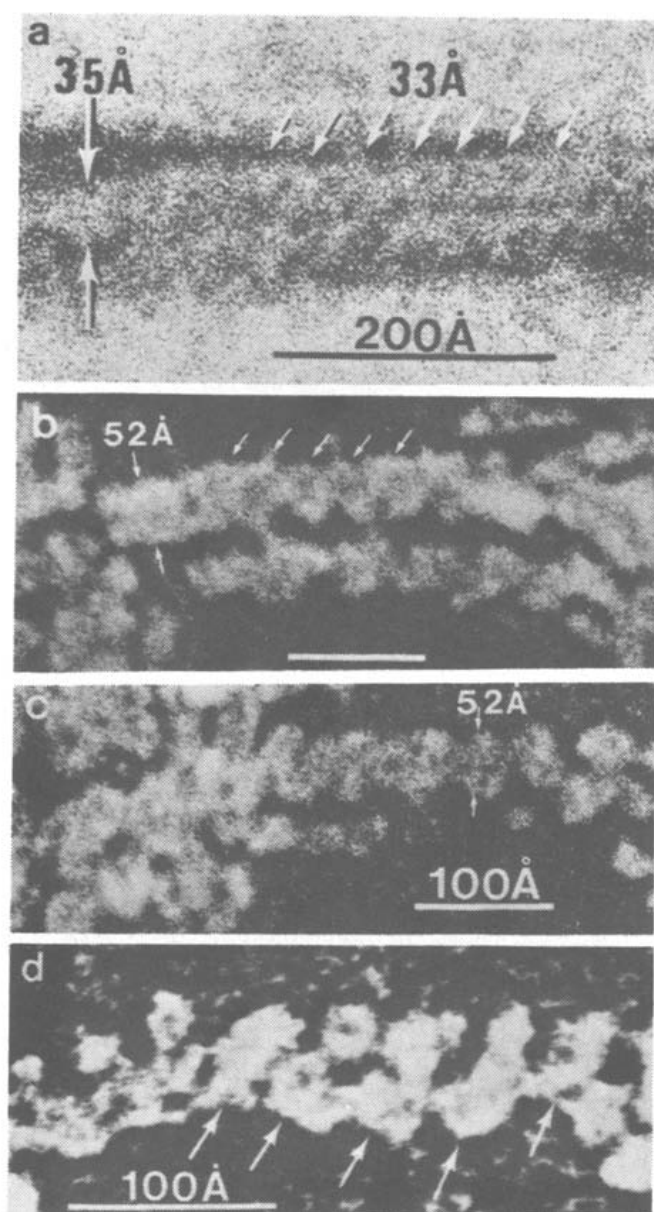


Fig 3 *A. xylinum* cellulose microfibrils (a) Treated with hot trifluoroacetic acid to remove hemicellulose, and negatively stained with 2% uranyl acetate. The upper microfibril averages  $35 \text{ \AA}$  in width and shows left-handed surface striations at approximately  $33 \text{ \AA}$  intervals. (b and c) Native microfibrils, freeze-dried and coated with  $17.3 \text{ \AA}$  Pt-C, bar,  $100 \text{ \AA}$ . (d) Pellicle material was boiled in trifluoroacetic acid, freeze-dried, and coated with  $15.2 \text{ \AA}$  Pt-C. Microfibril has been slightly opened up, so it clearly shows left-handed twists of the submicrofibrils as they wrap around the fiber axis.

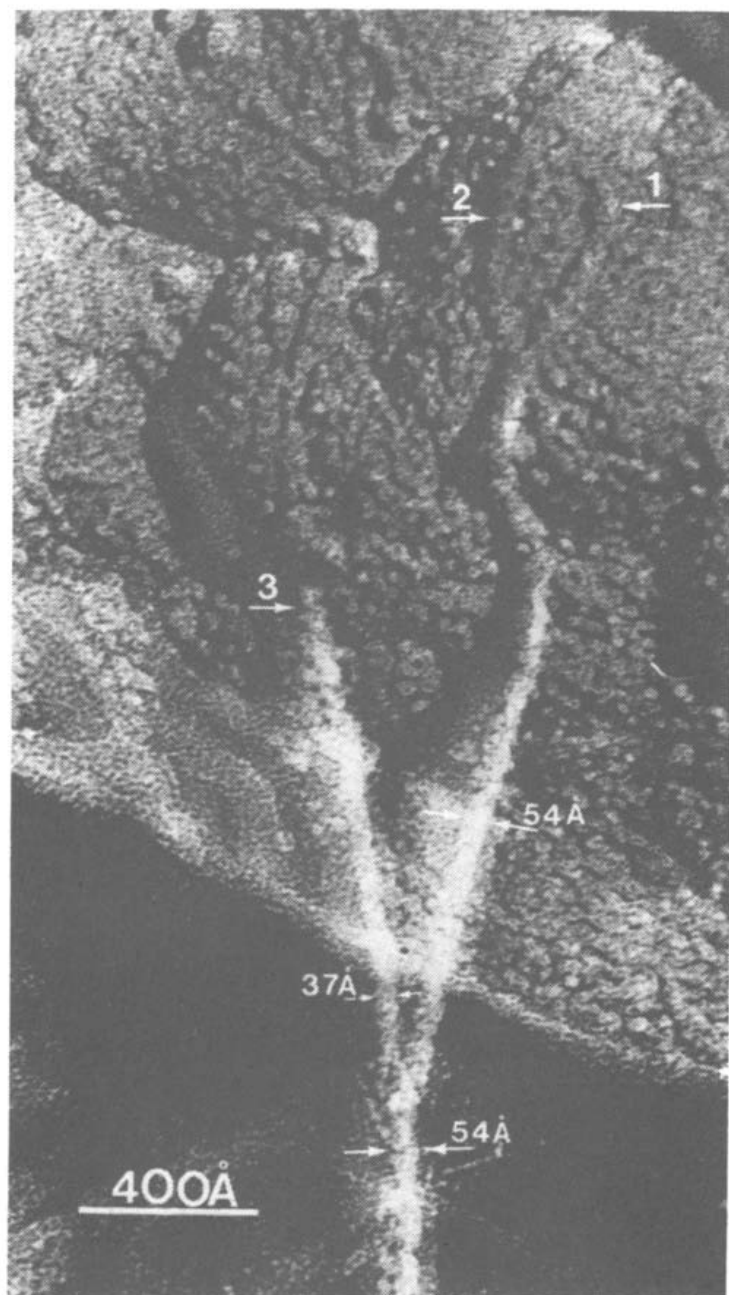


Fig. 4. Assembly of triple-stranded microfibril at surface of *A. xylinum* cell Pt-C (17.8 Å thick) coated submicrofibrils 1 and 2 join, making a Pt-C-coated, double fiber of 54 Å (37.6 Å, Pt-C corrected diameter). A third Pt-C-coated submicrofibril, 3, (supercoiled) of 37 Å (~20.6 Å, Pt-C corrected diameter) joins two submicrofibrils, producing a Pt-C-coated microfibril of ~54 Å (real size, 37.6 Å). This microfibril is not formed by lateral fasciation<sup>2,3,8,16</sup> along cellulose I crystal-lattice planes, but by twisting two  $17.8 \pm 2.2$  Å submicrofibrils together and wrapping a third  $17.8 \pm 2.2$  Å submicrofibril into the groove between them.

c.p.-m.a.s. n.m.r. spectrum<sup>27</sup> (see Fig. 2(c)) and by an electron-diffraction pattern<sup>6,28</sup> (see Fig. 2(b)), which shows the expected equatorial spacings<sup>29</sup> of approximately 6 Å, 5.3 Å, and 4 Å) that pellicle-material carbohydrate is 96.8% D-glucose<sup>30</sup> (see Fig. 2(a)) and is of the native, cellulose I, crystal form. Fig. 3(a) shows a negatively stained *A. xylinum* 35-Å cellulose microfibril with a left-handed-band structure occurring roughly at intervals of 33 Å. Although this same 33-Å banding pattern can be seen in Fig. 3(b) (arrows) on a 36.8 Å microfibril (corrected for a 17.3 Å Pt-C film), the microfibril directly below it and the one in Fig. 3(c) show irregular, left-handed banding. From such freeze-dried *A. xylinum* cellulose microfibril images as those in Fig. 3(b) and 3(c), we conclude that the microfibril is not a regular, helical structure. When the microfibril (see Fig. 3(d)) has been slightly

denatured in boiling trifluoroacetic acid, the left-handed, helicoidal structure is opened up, and the Pt-C-coated ( $15.2 \text{ \AA}$  thick) submicrofibrils averaging  $31.5 \text{ \AA}$  are seen ( $17.8 \text{ \AA}$  actual width).

In Fig. 4, *A. xylinum* grown normally after being grown on Tinopal<sup>13</sup> was freeze-dried (3 h at  $-70^\circ$ ), Pt-C-replicated ( $16.4 \text{ \AA}$  thick), and carbon-film backed. The replica was photographed at tilt intervals of  $10^\circ$  at  $10^5$  magnification, so it could be viewed stereoscopically<sup>22</sup>. This picture, one of the series, shows the formation of a three-stranded microfibril. At the upper right, submicrofibrils 1 and 2 are twisted together left-handedly (2 crossing over 1) having a Pt-C width of  $\sim 54 \text{ \AA}$ . Then, submicrofibril 3, which appears to be left-hand supercoiled, twists left-handedly (3 crosses over 1 and 2) around these two coiled submicrofibrils. This process gives rise to the observed  $32.5 \pm 2.1 \text{ \AA}$  submicrofibril banding interval and produces a Pt-C-coated microfibril of  $\sim 54 \text{ \AA}$  ( $39.1 \text{ \AA}$  real size).

The left-handed, triple submicrofibril construction is seen in bundled and primary cell-wall microfibrils in tobacco, as well as in the pellicle of *A. xylinum*. This mode of microfibril construction is incompatible with lateral fasciation or fusion of adjacent microfibrils or submicrofibrils along corresponding crystal-lattice

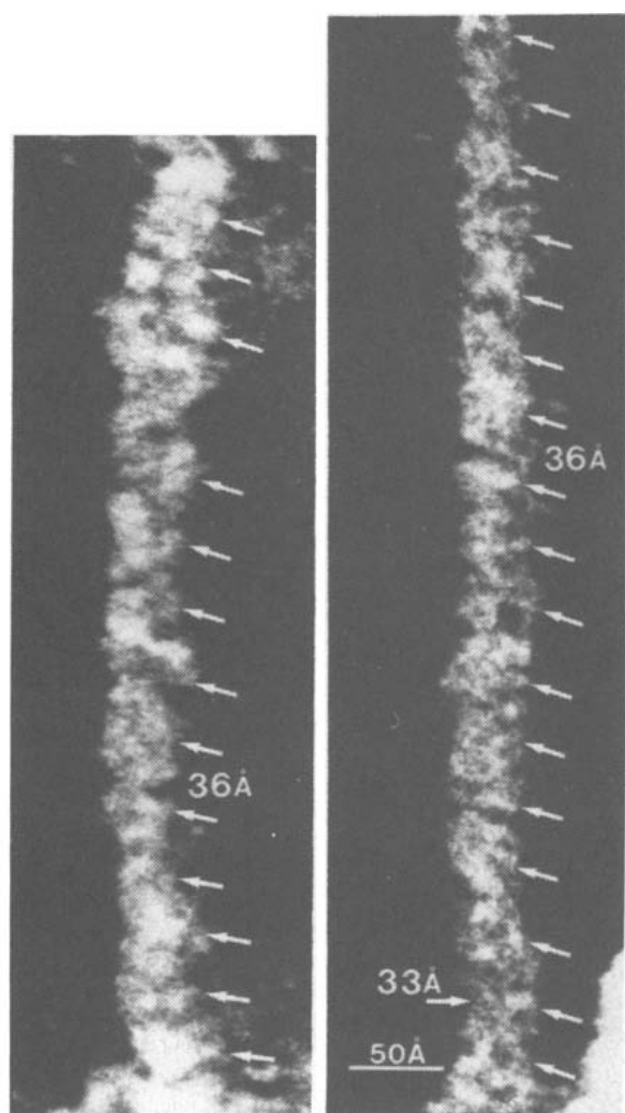
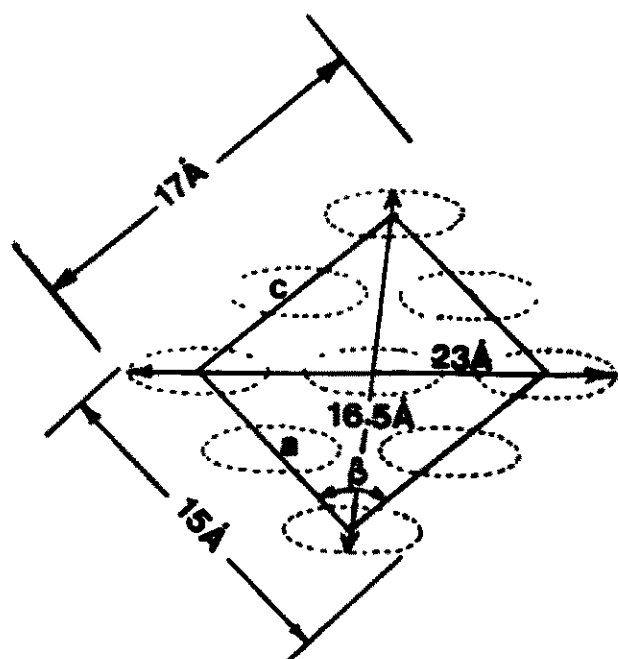


Fig 5 Sections of two submicrofibrils ( $33 \text{ \AA}$  Pt-C-coated,  $17.8 \pm 2.2 \text{ \AA}$  real diameter) showing left-handed surface striations of  $36 \text{ \AA}$ . *A. xylinum* was grown in  $0.25 \text{ mM}$  Tinopal, which disrupts microfibril formation<sup>6,13,14</sup>, and was freeze-dried, replicated with  $16.4 \text{ \AA}$  Pt-C, and backed with carbon



planes<sup>2,3</sup> to form microfibrils of 30–200 Å, as has been generally assumed<sup>2,4–6,14</sup>. A more likely mechanism for microfibril bundling probably occurs by hydrogen bonding of hemicelluloses (xylose content, see Fig. 2(a)) to adjacent microfibrils. This concept is supported by biochemical evidence<sup>1</sup>. The  $17.8 \pm 2.2$  Å submicrofibril we see must correspond to the primary fibrillar cellulose product ( $17 \pm 2$  Å wide) of a recently solubilized cellulose synthase from *A. xylinum*<sup>20</sup>. This supports previous findings<sup>6,14</sup> that the self-assembly process illustrated in Fig. 4 makes the 36.8 Å microfibril a secondary product of cellulose synthesis. By visibilizing the  $17.8 \pm 2.2$  Å submicrofibrils produced by *A. xylinum* grown on ~0.25mm Tinopal, which prevents microfibril formation, we have seen (see Fig. 5) a regular, left-handed surface striation which corresponds to the half spacing (36 Å) of the 72 Å, left-handed helix previously suggested for the packing structure of the (1→4)-β-D-glucan chains<sup>31</sup>. These spacings are also seen in the optical diffraction pattern in Fig. 1(e). These observations indicate that *A. xylinum* synthesizes left-handed-helical submicrofibrils which probably rotate in a left-handed direction during synthesis as they increase in length. It is probable that such a left-handed submicrofibril rotation is the driving force for the self-assembly of the three-stranded, left-hand-twisted  $36.8 \pm 3$  Å microfibril at the exterior surface of *A. xylinum*. The cellulose I fiber diffraction unit cell (orthogonal cross-section to the D-glucan chain longitudinal axis; see Fig. 6) derived by Ellis and Warwicker<sup>32</sup> ( $a = 10.85$  Å,  $b = 10.3$  Å,  $c = 12.08$  Å,  $\beta = 93^\circ 14'$ ), which contains 4 D-glucan chains that encompass



$$a = 10.85 \text{ Å}, b = 10.3 \text{ Å}, c = 12.08 \text{ Å}, \beta = 93^\circ 14'$$

Fig. 6. Schematic representation of the crystalline four (1→4)-β-D-glucan cellulose I unit cell, shown in an orthogonal cross section to its long axis or  $b$  axis. Because the unit cell is the repeating unit derived from X-ray fiber diffraction results, it is drawn through the centers of the D-glucan chain cross-sections. In contrast, TEM imaging would visibilize the exterior dimensions of the unit cell (assuming it is the submicrofibril) which encompasses nine (1→4)-β-D-glucan chains, and which has diagonal ( $d_1$  and  $d_2$ ) and side ( $s_1$  and  $s_2$ ) dimensions estimated from the unit-cell parameters printed in the Figure. An average diameter of the unit cell would measure 17.9 Å (the average of the sides and diagonals) and would agree with the  $17.8 \pm 2.2$  Å values which is the submicrofibril diameter measured by TEM and corrected for its Pt-C coating (see Experimental section)



a total of 9 D-glucan chains, probably corresponds to our submicrofibril. The dimensions,  $s_1 = 15 \text{ \AA}$ ,  $s_2 = 17 \text{ \AA}$ ,  $d_1 = 16.5 \text{ \AA}$ , and  $d_2 = 23 \text{ \AA}$  (17.9  $\text{\AA}$  average diameter), estimated from unit-cell dimensions in Fig. 6, corresponds to the average submicrofibril width of  $17.8 \pm 2.2 \text{ \AA}$  measured by TEM. The four-D-glucan-chain unit-cell is the only unit cell compatible with a left-handed, helical structure, as it was derived by assuming only that the (1 $\rightarrow$ 4)- $\beta$ -D-glucan chain are parallel<sup>32</sup>. The two D-glucan chains<sup>33</sup> ( $s_1 = 10 \text{ \AA}$ ,  $s_2 = 15 \text{ \AA}$ ,  $d_1 = 15 \text{ \AA}$ , and  $d_2 = 17 \text{ \AA}$ ; 14.2  $\text{\AA}$  average diameter) and the eight-chain unit cell<sup>2,3,34</sup> ( $s_1 = 17 \text{ \AA}$ ,  $s_2 = 23 \text{ \AA}$ ,  $d_1 = 28 \text{ \AA}$ , and  $d_2 = 30 \text{ \AA}$ ; 24.5  $\text{\AA}$  average diameter) are both strictly derived by assuming a straight D-glucan chain morphology, are smaller or larger than our measured submicrofibril average diameter, and do not fall within the  $17.8 \pm 2.2 \text{ \AA}$ , 95% fractile uncertainty.

Our observations do not support the accepted models of crystalline cellulose packed as straight chains that also fasciate laterally to form microfibrils of a range of sizes. Our results clearly show that the  $17.8 \pm 2.2 \text{ \AA}$  submicrofibril (the crystalline unit of cellulose which corresponds to the four D-glucan-chain fiber diffraction unit-cell) and the  $36.8 \pm 3 \text{ \AA}$  microfibril are uniquely related, and maintain their size and structural identities in native cellulose I.

#### ACKNOWLEDGMENTS

We thank Philip Morris for supporting this work, J. B. Wooten for the <sup>13</sup>C-c.p.-m.a.s. n.m.r. spectrum, W. S. Ryan, Jr., for his chemical work on *A. xylinum*, W. Krakow for the optical diffraction, N. J. Jacobs for culturing the *A. xylinum*, the Dartmouth EM facility, and JEOL for access to a JEM 1200 instrument in Peabody, MA, for part of the microscopy.

#### REFERENCES

- 1 P. ALBERSHEIM, *Sci. Am.*, 232 (1975) 81-95.
- 2 K. H. GARDNER AND J. BLACKWELL, *Biopolymers*, 13 (1974) 1975-2000.
- 3 H. SARKO AND R. MUGGLI, *Macromolecules*, 7 (1974) 486-494.
- 4 R. D. PRESTON, *The Physical Biology of Plant Cell Walls*, Chapman and Hall, London, 1974.
- 5 I. NIEDUSZYNSKI AND R. D. PRESTON, *Nature (London)*, 225 (1970) 274.
- 6 C. H. HAGLER AND M. BENZIMAN, in R. M. BROWN (Ed.), *Cellulose and Other Natural Polymer Systems*, Plenum, New York, 1982, pp. 273-297.
- 7 D. DELMER, *Adv. Carbohydr. Chem. Biochem.*, 41 (1983) 105-153.
- 8 J. MANLEY, *Nature (London)*, 204 (1964) 1155-1157.
- 9 A. N. J. HEYN, *J. Cell Biol.*, 29 (1966) 181-197.
- 10 I. OHAD, M. D. DANON, AND S. HESTRIN, *J. Cell Biol.*, 12 (1962) 31-46; I. OHAD AND M. D. DANON, *ibid.*, 22 (1963) 302-305.
- 11 A. FREY-WYSSLING AND K. MUHLETHALER, *Makromol. Chem.*, 62 (1963) 25-30.
- 12 K. ZAAR, *Cytobiologie*, 16 (1977) 1-15.
- 13 R. M. BROWN, JR., C. H. HAGLER, J. SUTTIE, A. R. WHITE, E. ROBERTS, C. SMITH, T. ITOH, AND K. COOPER, *J. Appl. Polym. Sci., Appl. Polym. Symp.*, 37 (1983) 33-78.
- 14 C. H. HAGLER, R. M. BROWN, JR., AND M. BENZIMAN, *Science*, 21 (1980) 903-906.
- 15 W. W. FRANKE AND B. ERMEN, *Z. Naturforsch.*, 24 (1969) 918-922.

- 16 R B HANNA AND W A COTE, *Cytobiologie*, 10 (1974) 102-116
- 17 H CHANZY, K IMADA, A MOLLARD, R VUONG, AND F BARNOUD, *Protoplasma*, 100 (1979) 303-316
- 18 A. FREY-WYSSLING, *The Plant Cell Wall*, Gebrüder Borntraeger, Berlin, Stuttgart, 1976 pp 97-101
- 19 G C RUBEN, K A MARX, AND T C REYNOLDS, *Annu. Proc. Elect. Microsc. Soc. Am.*, 39 (1981) 440-441
- 20 K A MARX AND G C RUBEN, *J. Biomol. Str. Dynam.*, 1 (1984) 1109-1132
- 21 G C RUBEN, *J. Elect. Microsc. Tech.*, 2 (1985) 53-57
- 22 G C RUBEN AND K. A MARX, *J. Elect. Microsc. Tech.*, 1 (1984) 373-385
- 23 G C RUBEN AND M W SHAFER, *Annu. Proc. Elect. Microsc. Soc. Am.*, 44 (1986) 448-449
- 24 G C RUBEN, G H BOKELMAN, AND H H. SUN, *Annu. Proc. Elect. Microsc. Soc. Am.*, 44 (1986) 206-207
- 25 G C RUBEN AND M W SHAFER, in C J. BRINKER, D E CLARK, AND D L ULRICH (Eds.), *Mat. Res. Soc. Symp. Proc.*, Palo Alto, CA, Better Ceramics Through Chemistry, II, 1986, pp 207-212
- 26 G C RUBEN AND K. A MARX, *Annu. Proc. Elect. Microsc. Soc. Am.*, 42 (1984) 684-685
- 27 D L VANDERHART AND R H ATALLA, *Macromolecules*, 17 (1984) 1465-1472
- 28 F C LIN, R M BROWN, JR, J B. COOPER, AND D P DELMER, *Science*, 230 (1985) 822-825
- 29 H J WELLAND, *J. Polym. Sci.*, 13 (1954) 471-476.
- 30 W S RYAN, *Beitr. Tabakforsch.*, 12 (1984) 105-111
- 31 A VSIWANATHAN AND S C SHENOUDA, *J. Appl. Polym. Sci.*, 15 (1971) 519-535
- 32 K. C ELLIS AND J O WARWICKER, *J. Polym. Sci.*, 56 (1962) 339-357
- 33 K H MEYER AND L MISCH, *Helv. Chim. Acta*, 20 (1937) 232.
- 34 R H MARCHESSAULT AND A SARKO, *Adv. Carbohydr. Chem.*, 22 (1967) 421-482